Experimental determination of the shear, rotational, and coupling viscosities for *p-n*-hexyl-cyanobiphenyl

T. Hirano* and K. Sakai

Institute of Industrial Science, University of Tokyo, 4-6-1, Komaba, Meguro-ku, Tokyo 153-8505, Japan
(Received 22 August 2007; published 14 January 2008)

In soft condensed materials consisting of molecules with form anisotropy, the translation and rotation interact with each other. Not only the shear and rotational viscosities but also the coupling viscosity are necessary to theoretically describe the molecular motion under coupling between the different degrees of freedom. In this paper, we report on the determination of all three viscosities with our experimental techniques. We obtained the absolute values for *p-n*-hexyl-cyanobiphenyl (6CB) in the isotropic phase. The experimental techniques used are the optical-beating spectroscopy of depolarized light scattering and the measurement of birefringence induced by capillary waves. The coupling strength is given in the form $2\mu^2/\eta\nu$ for the former and μ/ν for the latter; from this we determined the absolute values of η, ν, and μ. The coupling viscosity was found to be responsible for the critical behavior of the coupling effect reported previously.

I. INTRODUCTION

Shear flow in fluids consisting of anisotropic molecules, disklike, rodlike, and so on, can induce cooperative molecular rotations. On the other hand, the rotational motion of molecules causes macroscopic translational flow. Thus, the coupling between the shear and orientation plays an important role in the molecular motion. Some typical examples have been found in liquid crystals, even in the isotropic phase.

Three viscosity coefficients are usually defined to theoretically describe the molecular motion under the coupling between the two degrees of freedom. One is the shear viscosity η in the ordinary sense, and the others are the rotational viscosity ν with regard to the diffusion process of the rotational momentum, and the coupling viscosity μ concerned with the energy exchange between translation and rotation. While the value of η is easily measured with established methods, no reliable values of ν and μ have yet been acquired to our knowledge, because there have been no effective experimental techniques for their direct observation. The purpose of this study is to establish a method to determine all three coefficients.

The results are available in the form of ratios between these viscosities, and are different for each experiment. First, we observed the power spectra of depolarized light scattering [1,2]. Measuring the energy dissipation in the thermal equilibrium state, we obtain the coupling constant defined as $C_1 \equiv 2\mu^2/\eta\nu$. Our optical beating system has a very high frequency resolution, better than 1 kHz [3,4], and the coupling constant can be determined accurately even in the vicinity of the isotropic-to-nematic phase transition temperature [5]. Second, we observed the flow birefringence induced by the capillary waves [6]. The local orientational order induced by the shear deformation underneath the surface of a sample gives a coupling parameter defined as $C_2 \equiv \mu/\nu$. The system is shown to be effective for determining the absolute

value of C_2 as well as the shear viscosity η. Finally, quantitative estimations of ν and μ were also conducted.

II. COUPLING PARAMETERS

Three equations phenomenologically describe the motion of molecular degrees of freedom in fluids. One is Euler's formula, determining the translational motion,

$$\rho\dot{v}_i = \partial_j(\sigma_{ij} - p\delta_{ij}), \tag{1}$$

and the others are the constitutive equations that correlate the forces with the conjugate fluxes. When a molecule has large anisotropy in its shape, not only the shear stress and flow in the ordinary sense but also the rotational torque and motion must be considered. De Gennes proposed an additional term in the equations to represent the coupling between the two degrees of freedom, and succeeded in elucidating the extraordinary dynamics near the isotropic-to-nematic phase transition point [7]. We adopt the de Gennes expressions with fluctuation forces as follows:

$$\sigma_{ij} = 2\eta e_{ij} + 2\mu\dot{Q}_{ij} + \xi_\sigma, \tag{2}$$

$$\phi_{ij} = \nu\dot{Q}_{ij} + 2\mu e_{ij} + \xi_\phi, \tag{3}$$

where the shear stress σ_{ij} and the rotational torque ϕ_{ij} are linear combinations of the time evolution of each order parameter; e_{ij} is the shear rate, and Q_{ij} is the orientational order parameter. The free energy can be expanded in powers of Q around $Q=0$, the torque ϕ vanishes toward the virtual transition temperature T^*, and we obtain $\phi_{ij} = \delta F/\delta Q \approx a(T-T^*)Q_{ij}$, where a is a constant considered to characterize the molecular shape. The random thermal forces driving each degree of freedom are described by ξ_σ and ξ_ϕ.

A. Light-scattering spectra of orientational fluctuations

The fluctuation of the dielectric constant brought about by the thermal motion of various degrees of freedom in the material is observed with a light-scattering experiment. The thermal fluctuations drive the local shear flow and the rota-

*hirano22@iis.u-tokyo.ac.jp

tional motion of molecules evenly. The terms with respect to the thermal fluctuation in Eqs. (2) and (3) are characterized by $\langle \xi_\sigma(t)\xi_\sigma(0)\rangle = \langle \xi_\phi(t)\xi_\phi(0)\rangle = k_B T\delta(t)$ and $\langle \xi_\sigma(t)\xi_\phi(t')\rangle = 0$.

A spontaneous molecular orientation induces the microscopic anisotropy of the refractive index, and the power spectrum of the scattered light is related to the fluctuation of the orientational order Q_{ij} through the expression $S_{ij}(q,\omega)$

$= \int dt \, e^{-i\omega t}\langle \delta Q_{ij}(q,t)\delta Q_{ij}^*(q,0)\rangle$. We can measure the vertical-to-vertical (VV) component via the polarized light scattering and the vertical-to-horizontal (VH) component via the depolarized light scattering. The power spectra are given by [5]

$$S_{VV} = \frac{2\Gamma}{\omega^2 + \Gamma^2}, \tag{4}$$

$$S_{VH} = \frac{2\Gamma}{\omega^2 + \Gamma^2}\sin^2\frac{\theta}{2} + \frac{2\Gamma\left[\omega^2 + \left(\dfrac{\eta q^2}{\rho}\right)^2(1-C_1)\right]}{\left(\omega^2 - \dfrac{\eta q^2}{\rho}\Gamma\right)^2 + \omega^2\left[\Gamma + \dfrac{\eta q^2}{\rho}(1-C_1)\right]}\cos^2\frac{\theta}{2}, \tag{5}$$

where θ is the geometrical scattering angle.

The spectrum of the VV component is a quasielastic Lorentzian, and the half width at half maximum of the peak is written as $\Gamma = a(T-T^*)/\nu$, which corresponds to the inverse of the lifetime of the local orientation order. The VH component, on the other hand, is related to the off-diagonal factors of the dielectric tensor. A typical spectrum of Eq. (5) shows a Lorentzian curve with another Lorentzian peak subtracted. The outer peak stands for the process of orientational relaxation appearing also in the VV spectrum, while the inner dip represents the reorientation of molecules induced by the coupled shear flow. We obtain the coupling constant in the form $C_1 = 2\mu^2/\eta\nu$ consisting of three viscosity coefficients. Note here that C_1 is symmetric with respect to η and ν. In the thermal equilibrium state, coupling phenomena occur between the two evenly driven order parameters of the orientation and shear motion of the molecules. Accordingly, the rotation induced by the shear flow through the coupling is comparable to the original motion of the orientation.

B. Measurement of birefringence induced by capillary waves

In contrast to the observation of the thermal fluctuation of molecular orientation, we can observe the irreversible energy flow from one to the other degree of freedom in the measurement of birefringence induced by capillary waves.

The detail of the birefringence measurement under the shear flow induced by propagating capillary waves was reported previously [6]; here, we give a brief account. The oscillating vibration forced on a fluid surface excites the capillary wave. The dispersion relation is given by $\omega^2 = \gamma k^3/\rho$, where γ is the surface tension and ρ is the density. The velocity potential Φ describing the wave propagating along the x direction of a medium filling the half space of $z < 0$ is written as [8]

$$\Phi = \frac{A\omega}{k}e^{kz}e^{-i\omega t + (ik-\alpha)x}, \tag{6}$$

where A is the amplitude of the surface deformation and α is the spatial damping constant of the capillary wave, which is given by $\alpha = 4\eta\omega/3\gamma$.

The intensity of the external shear deformation is much larger than that of the thermal fluctuation, and we assume $\xi_\sigma(t) \propto e^{-i\omega t}$ and $\xi_\phi(t) \approx 0$ in Eqs. (2) and (3). A propagating wave accompanies the shear deformation roughly to a depth equal to the wavelength. Both the coupled orientation and the directly excited shear flow should be written as $Q_{ij}^* = Q_{ij}e^{-i\omega t}$ and $e_{ij}^* = e_{ij}e^{-i\omega t}$, and Eq. (3) can be solved to give Q_{ij} as

$$Q_{ij} = \frac{C_2}{i\omega - \Gamma}2e_{ij}. \tag{7}$$

The coupling coefficient C_2 is the ratio of μ and ν and independent of η, since the one-way flow of energy from the shear to the orientation modes is observed.

The absolute value of the orientation order Q is experimentally determined through the relation $Q = \Delta n/\Delta n_0$. Here, Δn_0 is defined as the difference between the anisotropic refractive indices for the ordinary and extraordinary rays in the perfectly ordered state and its literature value of 0.303 [9] is adopted. The anisotropy in the present experiment is obtained from the output signal of the lock-in amplifier through the equation

$$\Delta n = \frac{2\pi l}{\lambda \tan\theta}\frac{I_{out}}{I_0}, \tag{8}$$

where $l = 15$ mm is the effective width of the capillary wave, $\lambda = 633$ nm is the wavelength of the probe laser, $\theta = 3°$ is the initial retardation of the beam, and I_0 stands for the intensity of the beam through the analyzer without the capillary wave, which was measured in advance.

The absolute value of the shear rate caused by the surface wave is determined through the following relation:

$$e_{ij} = \frac{\partial}{\partial z}\frac{\partial\Phi}{\partial x}\left(= \frac{\partial}{\partial x}\frac{\partial\Phi}{\partial z}\right) \approx \omega A k e^{-\alpha x}e^{kz}. \tag{9}$$

We can estimate the surface deformation A from the gradient of the surface wave, which is determined by the deflection angle of the probe light with an optical lever technique.
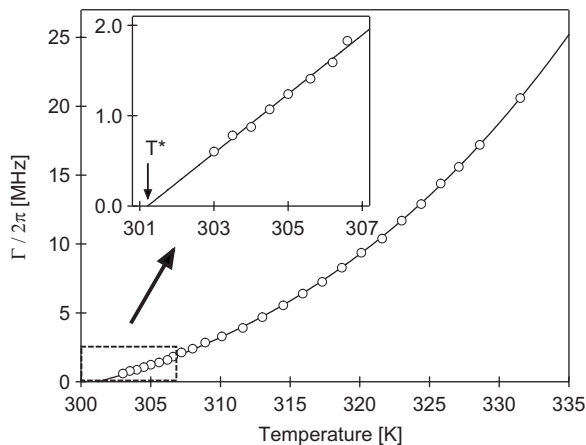
FIG. 1. Temperature dependence of the orientational relaxation frequency obtained from the VV component of the light-scattering spectra. The fitted curve represents the relation of Eq. (11). The inset shows the data near the I-N phase transition temperature.

Additionally, we obtain the following expression with respect to the fluid dynamics:

$$\rho \dot{v}_i = -\partial_i p + \eta \left(1 - C_1 \frac{i\omega}{i\omega - \Gamma} \right) \partial_i^2 v_i + \xi(t), \qquad (10)$$

by eliminating σ_{ij} and Q_{ij} from Eqs. (1)–(3). It is the Navier-Stokes equation with relaxing shear viscosity, which includes the effect of the shear-orientation coupling. The equation indicates that the apparent shear viscosity shows a single relaxation, with relaxation frequency Γ and strength C_1.

III. RESULTS AND DISCUSSION

In both the light-scattering and capillary-wave experiments, cyanobiphenyl-type liquid crystals are the best candidates for the samples because of their chemical and optical toughness and their well-known physical properties. We used p-n-hexyl-cyanobiphenyl (6CB) as the sample in this study because it has the lowest isotropic-to-nematic (I-N) phase transition temperature in the series of cyanobiphenyls. The sample was purchased from Merck and used without further purification. The sample cell was kept in a water jacket to control the sample temperature within an accuracy of 0.1 K. All the experiments were conducted for the isotropic phase near the I-N transition point.

We precisely measured the temperature dependence of the light scattering spectra for the VV and VH components. The results for nCB samples ($3 \le n \le 8$) have been reported in our previous paper [10]. Fitting the VV spectra with the theoretical Lorentzian curve of Eq. (4), we obtained the orientational relaxation frequency Γ, whose typical behavior for 6CB is shown in Fig. 1. The data obtained in the vicinity of T^* are also plotted in the inset of Fig. 1. They show good linear dependence on temperature, and T^* was determined as the intercept on the abscissa; consequently $\Gamma/2\pi = 0.326(T - T^*)$ MHz and $T^* = 301.2$ K were obtained. Additionally, the temperature dependence of Γ in a wide temperature range
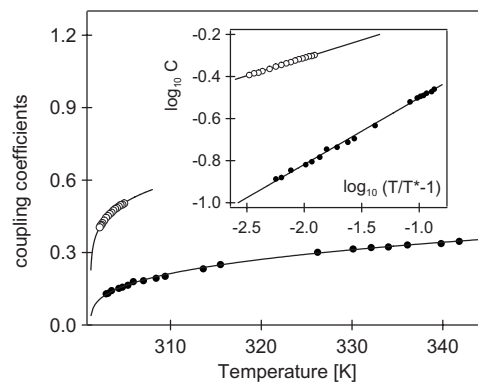

FIG. 2. Temperature dependence of both coupling coefficients C_1 (●) and C_2 (○). The inset is a double-logarithmic plot, which shows their critical behaviors toward T^*.

gives information on the activation energy of the rotational viscosity through the following expression:

$$\Gamma \propto \frac{T - T^*}{\exp(E_\nu / k_B T)}, \qquad (11)$$

where ν is supposed to follow the Arrhenius law similarly to other ordinary transportation coefficients. As a result of the curve fitting, the activation energy E_ν was determined to be $E_\nu / k_B = 2960$ K.

We determined the coupling constant C_1 by fitting the observed VH spectra with Eq. (5). The temperature dependence of C_1 thus obtained is shown in Fig. 2, where the inset shows its logarithmic plot. The critical behavior of C_1 vs temperature is suggested from the power law shown in the inset, and we obtained the relation $C_1 = 0.65(T/T^* - 1)^{0.32}$.

On the other hand, with the capillary-wave system, we observe capillary-wave propagation and oscillatory flow birefringence underneath the fluid surface. The temperature dependence of the orientation order for a certain magnitude of the shear deformation is then obtained. Figure 3 shows a typical spatial profile of birefringence obtained at 0.5 mm below the surface under the propagation of capillary waves at $\omega = 2\pi \times 80$ s^{-1}. The values of the wave number k and the damping constant α obtained as the fitting parameters of Eq.
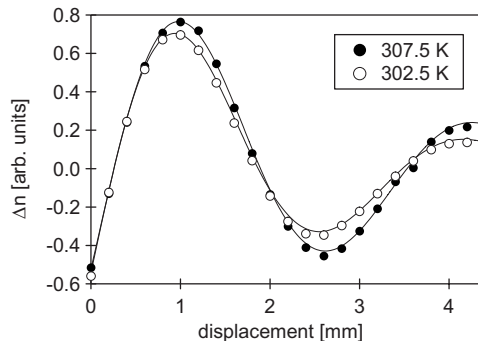

FIG. 3. Spatial profile of Δn in the direction of the propagating wave. The solid lines represent the fitted curves with the exponentially damping oscillation.

TABLE I. Experimental values of the surface tension and the shear viscosity determined and used in this study.

T (K)	307.5	306.1	305.0	304.0	303.0	302.3
γ (mN/m)	35.7	35.1	34.6	34.6	34.1	34.1
η (mPa s)	18.9	20.0	21.3	22.4	23.0	24.2

(6) gave those of the surface tension γ and the shear viscosity η. They are listed in Table I as functions of temperature.

Figure 4 shows an Arrhenius plot of the shear viscosity η, in which we can verify that the obtained values show the temperature dependence of $\eta = \eta_0 \exp(E_\eta/k_B T)$ with a single activation energy of $E_\eta/k_B = 4370$ K, and the limiting shear viscosity of $\eta_0 = 1.27 \times 10^{-8}$ Pa s.

To determine C_2, we simultaneously measured the absolute amplitude of the surface wave and the coupled orientation order underneath, cooling down the sample temperature gradually from 305 toward 302.2 K, which is the actual phase transition temperature to the nematic phase. Substituting the obtained values of Q_{ij} and e_{ij} and the values of Γ and T^* obtained by the light-scattering measurement into Eq. (7), we determined another coupling coefficient C_2. The result is shown in Fig. 2 together with C_1. Here, we can see the critical behavior of C_2 toward T^*, which is similar to that of C_1. We determined the critical exponent as the slope of the logarithmic plot shown in the inset and obtained the relation $C_2 = 1.07(T/T^* - 1)^{0.17}$.

Noticing the descriptions of C_1 and C_2, we naturally consider that the coupling viscosity is responsible for the critical behavior; the critical exponent of C_1 ($\propto \mu^2$) is twice the magnitude of that of C_2 ($\propto \mu^2$). We can then successfully determine the unique values of all the viscosities. Figure 5 shows the temperature dependences of the shear, rotation, and coupling viscosities, and the inset shows the critical behavior of μ together with the noncritical ones of η and ν.

Here, we determined the absolute value of each viscosity including its temperature dependence due to the critical and the Arrhenius behavior. In our previous study, we experimentally found that C_1 is almost independent of the temperature in a wide range far above T^* [2,10]. We concluded from this that the activation energy for η, ν, and μ should satisfy the

relation $E_\mu = (E_\eta + E_\nu)/2$. The activation energies E_ν and E_η are determined by the light-scattering and capillary-wave experiments, respectively, and then we can uniquely estimate E_μ from the above relation. The expressions for the three viscosities are given by

$$\eta = 1.27 \times 10^{-8} \exp(4370/T) \text{ Pa s},$$

$$\nu = 4.15 \times 10^{-7} \exp(2960/T) \text{ Pa s},$$

$$\mu = 4.08 \times 10^{-8}(T/T^* - 1)^{0.16} \exp(3670/T) \text{ Pa s}.$$

The orientation coupled with shear occurs more readily in the nematic than in the isotropic phase, and therefore it seemed reasonable that the coupling must become strong close to the nematic state. Our present data, however, show that the coupling coefficients C_1 and C_2 critically decrease and the coupling viscosity μ is the unique origin of their critical behaviors. The result indicates that the energy transfer via the coupling process decreases with decreasing temperature and becomes anomalously small in the neighborhood of the phase transition temperature.

This is probably due to the temperature dependence of the coherence length of the local orientation order [11], which is written as $\xi = \xi_0(T/T^* - 1)^{-0.5}$. While ξ is approximately as long as three molecular lengths at the highest temperature in our light-scattering experiment, it becomes several times as long at the critical region near T^*. The spontaneous close packing of anisotropic molecules for saving energy surpasses the disordering from the entropic effect within a domain. It is obvious that the coupling effect originates from anisotropy in the molecular shape or polarization. Instead, in the vicinity of the phase transition temperature, the temporal domain with the size ξ plays the role of a molecule because of the cooperative orientation in the domain. The anisotropy still remains in a small domain consisting of a few molecules; however, the form of the domain becomes spherelike with increasing size. The coupling viscosity would be expected to be meaningless for a spherical ensemble of molecules.
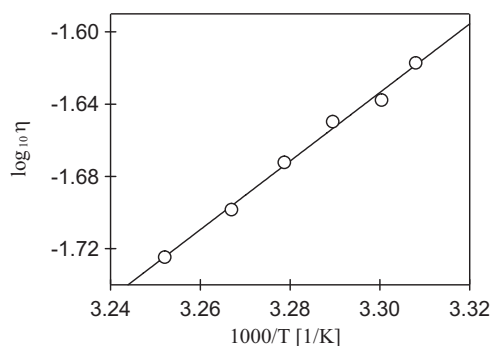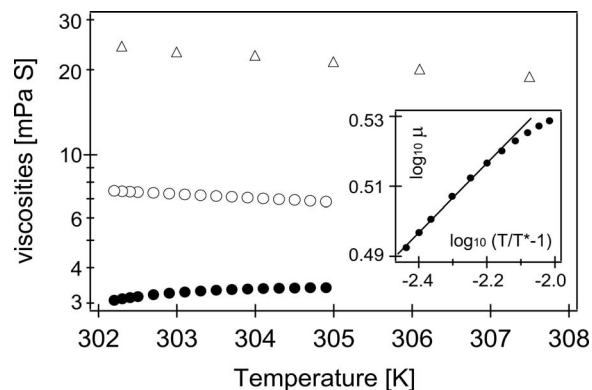

FIG. 4. Temperature dependence of the shear viscosity of 6CB determined by the damping of the capillary wave. The slope of the straight line gives the activation energy of η.

FIG. 5. Temperature dependence of the absolute values of the shear viscosity ($\triangle$), the rotational viscosity ($\bigcirc$), and the coupling viscosity ($\bullet$). The inset shows the logarithmic plot representing the critical behavior of μ.

Another plausible mechanism for decreasing μ is increase in the domain boundary. Energy loss through coupling (e.g., friction) might occur on the interface between neighboring domains. It is supposed that fewer domains in a certain volume possess less boundary area and thus lose less energy via the coupling process.

Nevertheless, we have no clear idea of the critical exponent of μ, determined to be 0.16 at present. The value may be a universal constant describing the I-N phase transition.

We will propose a further and more detailed model to clarify its physical meaning.

[1] G. R. Alms, D. R. Bauer, J. I. Brauman, and R. Pecora, J. Chem. Phys. **59**, 5304 (1973).

[2] G. R. Alms, T. D. Gierke, and G. D. Patterson, J. Chem. Phys. **67**, 5779 (1977).

[3] T. Matsuoka, K. Sakai, and K. Takagi, Rev. Sci. Instrum. **64**, 2136 (1993).

[4] K. Sakai, K. Hattori, and K. Takagi, Phys. Rev. B **52**, 9402 (1995).

[5] T. Matsuoka, K. Sakai, and K. Takagi, Phys. Rev. Lett. **71**, 1510 (1993).

[6] K. Sakai, M. Hosoda, and K. Takagi, Jpn. J. Appl. Phys., Part 1 **42**, 2935 (2003).

[7] P. G. de Gennes, Mol. Cryst. Liq. Cryst. **12**, 193 (1971).

[8] V. G. Levich, *Physicochemical Hydrodynamics* (Prentice-Hall, Englewood Cliffs, NJ, 1962).

[9] J. Li, S. Gauzia, and S.-T. Wu, Opt. Express **12**, 2002 (2004).

[10] T. Hirano, K. Takagi, and K. Sakai, Phys. Rev. E **72**, 041707 (2005).

[11] J. J. Stankus, R. Torre, C. D. Marshall, S. R. Greenfield, A. Sengupta, A. Tokmakoff, and M. D. Fayer, Chem. Phys. Lett. **194**, 213 (1992).